



Bacterial biofilm mechanical properties persist upon antibiotic treatment and survive cell death

K Zrelli, Olivier Galy, L Latour-Lambert, L Kirwan, J M Ghigo, Christophe Beloin, N Henry

► To cite this version:

K Zrelli, Olivier Galy, L Latour-Lambert, L Kirwan, J M Ghigo, et al.. Bacterial biofilm mechanical properties persist upon antibiotic treatment and survive cell death. *New Journal of Physics*, 2013, 15 (12), pp.125026. 10.1088/1367-2630/15/12/125026 . pasteur-01378684

HAL Id: pasteur-01378684

<https://pasteur.hal.science/pasteur-01378684>

Submitted on 10 Oct 2016

HAL is a multi-disciplinary open access archive for the deposit and dissemination of scientific research documents, whether they are published or not. The documents may come from teaching and research institutions in France or abroad, or from public or private research centers.

L'archive ouverte pluridisciplinaire **HAL**, est destinée au dépôt et à la diffusion de documents scientifiques de niveau recherche, publiés ou non, émanant des établissements d'enseignement et de recherche français ou étrangers, des laboratoires publics ou privés.



Distributed under a Creative Commons Attribution 4.0 International License

Bacterial biofilm mechanical properties persist upon antibiotic treatment and survive cell death

This content has been downloaded from IOPscience. Please scroll down to see the full text.

2013 New J. Phys. 15 125026

(<http://iopscience.iop.org/1367-2630/15/12/125026>)

View [the table of contents for this issue](#), or go to the [journal homepage](#) for more

Download details:

IP Address: 157.99.52.18

This content was downloaded on 10/10/2016 at 14:43

Please note that [terms and conditions apply](#).

You may also be interested in:

[Material properties of biofilms—a review of methods for understanding permeability and mechanics](#)

Nicole Billings, Alona Birjiniuk, Tahoura S Samad et al.

[Advances in the microrheology of complex fluids](#)

Thomas Andrew Waigh

[The physics of biofilms—an introduction](#)

Marco G Mazza

[Inactivation of Gram-positive biofilms by low-temperature plasma jet at atmospheric pressure](#)

F Marchal, H Robert, N Merbahi et al.

[Nanoindentation of Pseudomonas aeruginosa bacterial biofilm using atomic force microscopy](#)

Mahmoud Baniyasadi, Zhe Xu, Leah Gandee et al.

[Single particle tracking reveals spatial and dynamic organization of the E. coli biofilm matrix](#)

Alona Birjiniuk, Nicole Billings, Elizabeth Nance et al.

[Microrheology of complex fluids](#)

T A Waigh

Bacterial biofilm mechanical properties persist upon antibiotic treatment and survive cell death

K Zrelli¹, O Galy¹, P Latour-Lambert², L Kirwan³, J M Ghigo²,
C Beloin² and N Henry^{1,3,4}

¹ Laboratoire Physico-Chimie Curie (CNRS UMR 168), Institut Curie,
F-75231 Paris, France

² Institut Pasteur, Unité de Génétique des Biofilms, Département de
Microbiologie, F-75015 Paris, France

³ Laboratoire Jean Perrin (CNRS FRE 3231), UPMC, F-75252 Paris, France
E-mail: nelly.henry@upmc.fr

New Journal of Physics **15** (2013) 125026 (17pp)

Received 8 June 2013

Published 20 December 2013

Online at <http://www.njp.org/>

doi:10.1088/1367-2630/15/12/125026


Abstract. Bacteria living on surfaces form heterogeneous three-dimensional consortia known as biofilms, where they exhibit many specific properties one of which is an increased tolerance to antibiotics. Biofilms are maintained by a polymeric network and display physical properties similar to that of complex fluids. In this work, we address the question of the impact of antibiotic treatment on the physical properties of biofilms based on recently developed tools enabling the *in situ* mapping of biofilm local mechanical properties at the micron scale. This approach takes into account the material heterogeneity and reveals the spatial distribution of all the small changes that may occur in the structure. With an *Escherichia coli* biofilm, we demonstrate using *in situ* fluorescent labeling that the two antibiotics ofloxacin and ticarcillin—targeting DNA replication and membrane assembly, respectively—induced no detectable alteration of the biofilm mechanical properties while they killed the vast majority of the cells. In parallel, we show that a proteolytic enzyme that cleaves extracellular proteins into short peptides, but does not alter bacterial viability in the biofilm, clearly affects the mechanical properties of the biofilm structure, inducing a significant increase of the material compliance. We conclude that conventional biofilm

⁴ Author to whom any correspondence should be addressed.



Content from this work may be used under the terms of the [Creative Commons Attribution 3.0 licence](https://creativecommons.org/licenses/by/3.0/).
Any further distribution of this work must maintain attribution to the author(s) and the title of the work, journal citation and DOI.

control strategy relying on the use of biocides targeting cells is missing a key target since biofilm structural integrity is preserved. This is expected to efficiently promote biofilm resilience, especially in the presence of persister cells. In contrast, the targeting of polymer network cross-links—among which extracellular proteins emerge as major players—offers a promising route for the development of rational multi-target strategies to fight against biofilms.

 Online supplementary data available from stacks.iop.org/NJP/15/125026/mmedia

Contents

| | |
|--|-----------|
| 1. Introduction | 2 |
| 2. Materials and methods | 4 |
| 2.1. Chemicals, media, strains | 4 |
| 2.2. Biofilm growth and magnetic probe seeding | 4 |
| 2.3. Biofilm treatments and labeling | 4 |
| 2.4. Magnetic force setup | 5 |
| 2.5. Particle imaging and tracking | 5 |
| 2.6. Microrheology analysis | 5 |
| 2.7. Confocal imaging | 6 |
| 3. Results | 6 |
| 3.1. Biofilm mechanical profiles | 6 |
| 3.2. Antibiotic treatment | 8 |
| 3.3. Protease effect on biofilm mechanics | 11 |
| 4. Discussion and conclusions | 13 |
| References | 16 |

1. Introduction

Although our understanding of bacterial biofilm molecular biology has markedly increased recently, the development of these complex and fascinating living assemblages still raise a number of fundamental and practical questions. Rational strategies to control their development, maintenance or removal are still rare, calling for a deeper understanding of the causal relationships linking their physical, chemical and biological properties. For this purpose, an integrated and comprehensive description of biofilm mechanical properties is necessary. The challenge is not only to bring about new ideas for the physical control of biofilms, but also to find the mainspring of the material's mechanical behavior and eventually clarify the role of the physical cues in biofilm specific lifestyle. The heterogeneity and the highly dynamical nature of the biofilm material seriously hinders this enterprise. During the last decade, the question of bacterial biofilm mechanical properties has been addressed by several groups using a variety of methods such as the analysis of biofilm streamer deformations due to variations in fluid flow rates (Stoodley *et al* 1999, Klapper *et al* 2002), uniaxial compression of biofilm pieces lifted from agar medium or grown on cover slides (Korstgens *et al* 2001, Cense *et al* 2006), shearing of biofilm collected from the environment and transferred to a parallel plate rheometer (Towler *et al* 2003, Shaw *et al* 2004), atomic force microscopy using a glass

bead coated with a bacterial biofilm attached to an AFM cantilever (Lau *et al* 2009) or a dedicated microcantilever method for measuring the tensile strength of detached biofilm fragments (Poppele and Hozalski 2003, Aggarwal *et al* 2010). These approaches have produced a large range of elastic moduli, viscosities or cohesion forces that differ by several orders of magnitude. Discrepancies observed in the literature originate in part from important differences in the biological material investigated across the various studies and in the experimental approaches involving disparate force and time scales as well as calculation methods (Aravas and Lapidou 2008). In addition, authors have also recognized large variations in data sets stemming from the same consistent investigations (Brindle *et al* 2011) and conceded to both technical difficulties and biofilm inherent variability. In this context, a general agreement about the visco-elastic nature of bacterial biofilms has emerged but the large dispersion of the values usually obtained on biofilms removed from their native environment compromised further insights into the understanding of the fundamental components underpinning biofilm mechanical properties. Most investigators have considered biofilms as homogeneous materials and therefore analyzed mechanical responses averaged over the whole material, whereas almost all biofilm characteristic properties such as biomass, concentration of chemicals or gene expression measured at the micron scale were shown to exhibit strongly heterogeneous spatial distribution (Stewart and Franklin 2008). To address the question of the biofilm mechanical heterogeneity, we recently introduced a biofilm-microrheology experiment directed to measuring *in situ* the biofilm mechanical properties at the micron scale and mapping out their spatial distribution. The principle of the experiment consists of remote actuation of micrometric magnetic particles seeded in a growing biofilm using a dedicated magnetic tweezer setup. Using this new tool with *Escherichia coli* biofilms, we were able to measure the three-dimensional (3D) spatial distribution of their visco-elastic parameters and to demonstrate their heterogeneity, collecting values spreading over almost three orders of magnitude in the same biofilm. Thereby, we have demonstrated the clear-cut effect of cell surface appendages and environmental conditions on the mechanical properties of biofilms (Galy *et al* 2012).

Here, we raise the question of the effect of antibiotics on biofilm mechanical properties. This problem is not only relevant to the design of biofilm control strategies but also to a better understanding of the molecular features supporting biofilm mechanical properties. Indeed, finding effectors altering these properties should help to identify their bases. Moreover, biofilms have been shown to build up significant strong multifactorial resistance to antibiotic treatment (Stewart and Costerton 2001, Anderson and O'Toole 2008, Hoiby *et al* 2010) but the potential role of physical factors in these processes is still poorly understood. Mainly based on semi-quantitative evaluation, previous studies addressing this question have not brought out a definitive picture of the effects of antibiotics on biofilm mechanics. On the basis of macroscopic rheometry data, Lieleg and co-workers examined several *Pseudomonas* biofilms and have concluded to the absence of the effect of antibiotics (Lieleg *et al* 2011), while in another investigation, the authors found that ciprofloxacin and rifampicin weakened *P. aeruginosa* and *S. epidermidis* biofilms (Jones *et al* 2011). However, there is a concern that scrapping and pooling of the biofilm before transfer to the rheometer could have blurred potentially induced changes. The purpose of the work reported here is to take advantage of the detailed information provided by the remote actuation of magnetic particles in a biofilm maintained in its native environment, to reconsider the question of the effect of antibiotics on biofilm physical properties and to collect information useful to the recognition of the molecular factors contributing to biofilm physical properties.

We conducted this study in a model biofilm formed by an *E. coli* strain carrying a derepressed conjugative plasmid F and producing *F pilus*, a surface appendage that promotes bacterial adhesion and biofilm formation (Ghigo 2001). In order to test the effect of two antibiotics holding different mechanisms of action we used ofloxacin, known to inhibit DNA gyrase, and ticarcillin, known to prevent cross-linking of peptidoglycan during cell wall synthesis. We describe here the mechanical profile of a reference biofilm grown under a controlled nutrient flow before and after antibiotic treatment. In parallel, we probed *in situ* bacterial mortality induced by the antibiotic using a cell death fluorescent marker. To endorse the antibiotic results and gain further insight into the understanding of the biofilm mechanics, we also assessed the effect on biofilm mechanics induced by the proteolytic enzyme, trypsin.

We compare the impact of antibiotic and protease on biofilm physical characteristics and conclude that biofilm mechanics are strongly resistant to antibiotic treatment. We also propose a crucial role for extracellular proteins in the *E. coli* biofilm structural organization. These results support the idea already proposed by others of a distinction between cell killing power and biofilm elimination efficiency of antibiotics. Eventually, we analyze the consequences of our findings for the development of new biofilm control strategies.

2. Materials and methods

2.1. Chemicals, media, strains

Tetracycline, ticarcillin (Ticarpen[®]) was from GlaxoSmithKline (Marly-le-Roi, France) and ofloxacin from Sigma-Aldrich (France). Propidium iodide (PI) and magnetic beads (Dynabeads M-270 Amine) were purchased from Life Technologies (France).

Bacteria were grown in lysogeny broth medium and in defined M63B1 medium with 0.4% glucose (M63B1Glu). We used isogenic *E. coli* bacterial strains carrying a derivative of the F-conjugative plasmid (F'tet) (Ghigo 2001) and constitutively producing green fluorescent protein (GFP), MG1655_ampgfp_F'tet (Tet^R, Amp^R) and MG1655_kmgfp_F'tet (Tet^R, Km^R). Minimum inhibitory concentration (MIC) values of ticarcillin and ofloxacin were taken equal to be 1 and 0.0625 $\mu\text{g ml}^{-1}$, respectively (Bernier *et al* 2013).

2.2. Biofilm growth and magnetic probe seeding

Bacteria grown in the presence of tetracycline 7.5 $\mu\text{g ml}^{-1}$ at 37 °C, taken in the exponential phase were introduced at OD = 0.05 in a 800 μm side length internal side and 160 μm wall thickness capillaries (Composite Metal Services, Shipley, UK) at the same time as the magnetic particles, 2.8 μm in diameter, at a final concentration of $2.5 \times 10^6 \text{ ml}^{-1}$. The mixed suspension was allowed to sediment under static conditions for 1 h before starting the flow for the entire growth period. Continuous flow was applied using a push-pull syringe pump which delivered a 0.3 ml h^{-1} laminar flow (Reynolds number below 2) and an approximate wall shear 10^{-3} Pa .

2.3. Biofilm treatments and labeling

2.3.1. Enzymatic and antibiotic treatment. Antibiotics—ofloxacin and ticarcillin—and enzyme were soaked through the biofilm by adding the required concentrations in the medium flow—M63B1 medium containing glucose—at 37 °C from time t_i , generally 24 h after biofilm initiation, to final incubation time, t_f .

2.3.2. Propidium iodide. PI 20 μ M was introduced in the biofilm from flow circuit outlet enabling flow inversion during the time necessary for the counterflow to reach the capillary. Then the flow was stopped for 5 min and the capillary was imaged before re-starting the nutrient flow forward.

2.4. Magnetic force setup

Magnetic tweezers were set up as detailed in a previous paper (Galy *et al* 2012). Briefly, two magnetic poles, each made of a copper coil with 2120 turns of 0.56 mm in diameter copper wire and soft magnetic alloy cores (Supra50-Arcelor Mittal, France) were mounted on an inverted Nikon TE-300 microscope, north pole facing south pole, in order to generate a magnetic force in one direction along the length of the capillary. In order to determine the absolute force acting on the beads embedded in the biofilm, we measured the velocity of beads dispersed in a purely viscous mixture of glycerol and water (39.8 g in 200 μ l water). We derived the force from Stokes' law neglecting the inertia of the particles and checked linear dependence between force and current. The variation in the force with the distance to the poles was taken into account by recording the particle trajectories in the entire volume of interest, and storing the velocities with their coordinates (x_i , y_i , z_i) in a calibration file which was used to derive visco-elastic parameters from particle displacement curves in the biofilm. The amplitude of force in the zone of interest varied from 29 pN in microvolumes most distal from the poles at the center of the capillary to 104 pN at the side walls of the capillaries near the pole pieces. The linearity of the visco-elastic response at applied forces ranging from 20 to 100 pN was verified. As well, superimposed creep curves were obtained when the same force was applied successively on the same particle.

2.5. Particle imaging and tracking

Particles in the biofilm were imaged in the capillary using a Nikon S Fluor $\times 40$ objective (NA 0.9, WD 0.3) and an electron multiplying charge coupled device (EMCCD) camera (C 9100-02, Hamamatsu Photonics). Particles were imaged using their large-spectrum intrinsic fluorescence signal (filters Exc 540/25 nm; DM 565; Em 605/55). To monitor particle motion upon magnetic force application, image sequences were recorded at a frequency of 30 Hz over a period of 20 s and further analyzed using an ImageJ particle tracker, as developed by Sbalzarini and Koumoutsakos (2005), that yielded particle trajectories from which individual particle creep curves giving material strain versus time could be plotted. The error made on the particle position was evaluated by monitoring the position of the resting beads and found to be equal to 0.02 μ m.

2.6. Microrheology analysis

Material compliance was derived from particle motion as previously established for a probe particle of radius R embedded in an incompressible, homogeneous visco-elastic medium (Schnurr *et al* 1997), which gives the time-dependent creep compliance of the network $J(t)$ (equal to the reciprocal macroscopic shear modulus), knowing probe deflection $d(t)$ and applied force f as follows:

$$J(t) = d(t) \times \frac{6\pi R}{f}. \quad (1)$$

Next, we extracted the visco-elastic moduli by fitting the creep curves to the time-dependent visco-elastic behavior of Burger's model—an equivalent mechanical circuit made of a spring and a dashpot combined in parallel and a second spring and dashpot added in series—as classically done to quantify visco-elastic materials, but also more complex and biological polymer rheological properties (Bausch *et al* 1998, Jones *et al* 2011). The results were analyzed according to the corresponding analytical solution as follows:

$$J(t) = J_0 + J_1 (1 - e^{-t/\tau}) + \frac{t}{\eta_0}, \quad (2)$$

where J_0 is the elastic instantaneous compliance, τ is the relaxation time required for the transition from the elastic to the viscous regime, J_1 gives the amplitude of elastic relaxation and η_0 measures the effective viscosity of the material.

Boundary conditions were evaluated using the theoretical approach of Perkins and Jones (1991, 1992) for both hard wall and free surface effects. The correction function was calculated to the fifth order and taken into account to correct particle velocity in the capillary in the limit of 20% correction, i.e. from 4 μm from the bottom of the capillary to 3 μm from the free surface. Particles located outside of these limits were not taken into account in the analysis.

2.7. Confocal imaging

Confocal microscopy images were acquired using a Leica TCS SP5 AOBS inverted confocal laser scanning microscope equipped with HCX PL Apo 63x/1.4-0.6 Oil immersion objective lens. We monitored cell GFP and PI fluorescence using 488 and 561 nm excitation wavelength, respectively, and collecting emission band-pass filters centered at 520/20 nm (GFP) and 640/60 nm (PI).

3. Results

3.1. Biofilm mechanical profiles

To establish a reference mechanical profile, we grew a typical biofilm using *F pilus* producing *E. coli* bacteria seeded with magnetic particles during 24 h under a continuous nutrient flow of 0.3 ml h⁻¹ providing an adherent bacterial layer of 30–40 μm height. Examples of particle spatial distribution in a plane are shown in figure 1(A). Local mechanical properties of the material were then probed by applying a 16 s force step on the particles dispersed in the three dimensions of the biofilm. The induced particle deflection recorded versus time was used to extract the visco-elastic parameters as previously shown (Galy *et al* 2012). Particle displacements reported heterogeneous local mechanical environments exhibiting responses differing both in shape and amplitude as shown in figure 1(B). Local responses were predominantly of a visco-elastic nature displaying elastic compliance (J_0), viscosity (η_0) and relaxation (J_1, τ) (see panel 1 in figure 1(B)). However, in 30 \pm 15% of the cases, the particles reported purely elastic behavior (see panel 2 in figure 1(B)). The spatial distribution of the mechanical parameters indicated that environments with elasticity and viscosity values differing from two orders of magnitude coexisted laterally and in the depth of the biofilm (see compliance values spatial distribution in figure S1 (available from stacks.iop.org/NJP/15/125026/mmedia)). A bottom layer extending to about 10 μm thickness close to the adhesive substrate exhibited lower values of compliance as well as lower spreading of the values or in other words higher

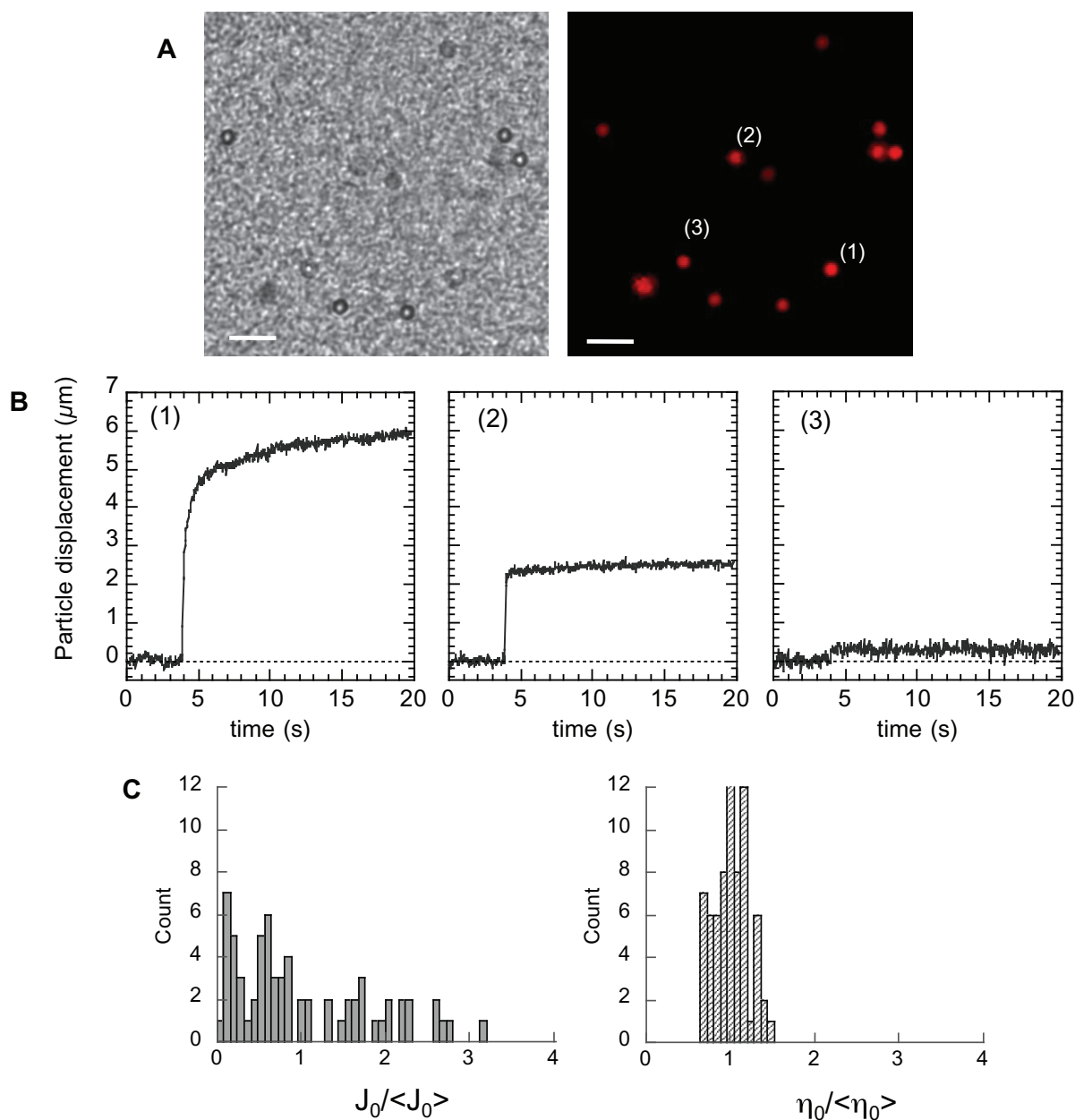


Figure 1. Typical *E. coli* biofilm mechanical property heterogeneity. (A) Pictures of a 24 h biofilm seeded with magnetic particles, bright field images (left) and fluorescence images (Exc 535/15 nm; Em 565/20 nm) (right); bar represents 10 μm . (B) Creep curves obtained upon magnetic force application; curves from the particles numbered on the microscope images. (C) Distribution of elastic compliance values normalized to the mean for a typical biofilm (left) and equivalent data obtained in glycerol (right).

stiffness and lower heterogeneity. Considering that all the particles tested reported elastic deformation of their environment, we focused our analysis on the elastic compliance (J_0). Figure 1(C) shows the distribution of J_0 values for the reference biofilm. The values have

Table 1. Parameters of the value distributions normalized to ensemble-average for glycerol—amplitude of the viscous flow over $(1/\eta_0)$ —and for the reference biofilm—elastic compliance (J_0) .

| Material | Median | Standard deviation |
|---|------------------|--------------------|
| Glycerol | 1.01 ± 0.005 | 0.038 ± 0.002 |
| <i>F. pilus</i> biofilm 0.3 ml h^{-1} —24 h | 0.7 ± 0.16 | 0.82 ± 0.1 |

\pm Std error.

been normalized to the ensemble average, enabling distribution characterization independently of the parameter itself and evaluation of the degree of heterogeneity of the material to be compared with the distribution of the values obtained in glycerol by the same technique of particle actuation (only viscous contribution as expected). In this case, the distribution displayed a completely different symmetrical shape centered on unit as expected from a typically homogeneous viscous liquid and a much lower standard deviation (see table 1). The spreading of the data obtained in glycerol also gave the experimental error of the measurements—much lower than the standard deviation of the data obtained in the biofilm. In this approach standard deviation of the data is directly related to the degree of heterogeneity of the sample.

Thus, the reference biofilm exhibited an the overall mechanical profile reporting a heterogeneous response dominated by an elastic deformation differing by two orders of magnitude in the three dimensions of the material, exhibiting a mean elastic compliance value of $0.4 \text{ m}^2 \text{ N}^{-1}$ and a standard deviation of $0.33 \text{ m}^2 \text{ N}^{-1}$ in good agreement with previous results we have obtained on similar biofilms grown at slightly different flow rates (Galy *et al* 2012).

3.2. Antibiotic treatment

3.2.1. Impact on biofilm mechanics. We next examined the alterations induced by antibiotic treatment on the mechanical properties of this reference biofilm. The experiments were conducted using ofloxacin, which inhibits DNA replication and ticarcillin which targets cell membrane. After having collected the creep curves of the particles embedded in a biofilm selected volume, we started antibiotic treatment at initial time $t = t_i$ by adding $50 \mu\text{g ml}^{-1}$ of ofloxacin or $800 \mu\text{g ml}^{-1}$ of ticarcillin to the nutrient flow that soaked through the biofilm. These antibiotic concentrations corresponded to 800 times the MIC obtained on planktonic cells. The treatment was maintained up to time $t = t_f$, i.e. after 12 h in the presence of ofloxacin and 20 h in the presence of ticarcillin. Then, the mechanical profile was recorded again in the same volume of the biofilm, tracking the deflection induced by the magnetic force for the same particles as the previous treatment. The same procedure was employed in parallel on control capillaries in the absence of an antibiotic. We observed that the antibiotic-treated biofilm's height stagnated while the control biofilm kept on growing and was higher by approximately $10 \mu\text{m}$ (data not shown). In all cases particle location in the xy plane showed very small changes and particles that had been tracked at t_i could be easily found again at t_f both in the treated samples and in the controls on the basis of their xy coordinates. Creep curves obtained at time t_i and t_f were used to derive elastic compliance differences $\Delta J_0 = (J_0(t_f) - J_0(t_i))$ particle per particle. The results displayed in figure 2 show typical distributions obtained after 12 and

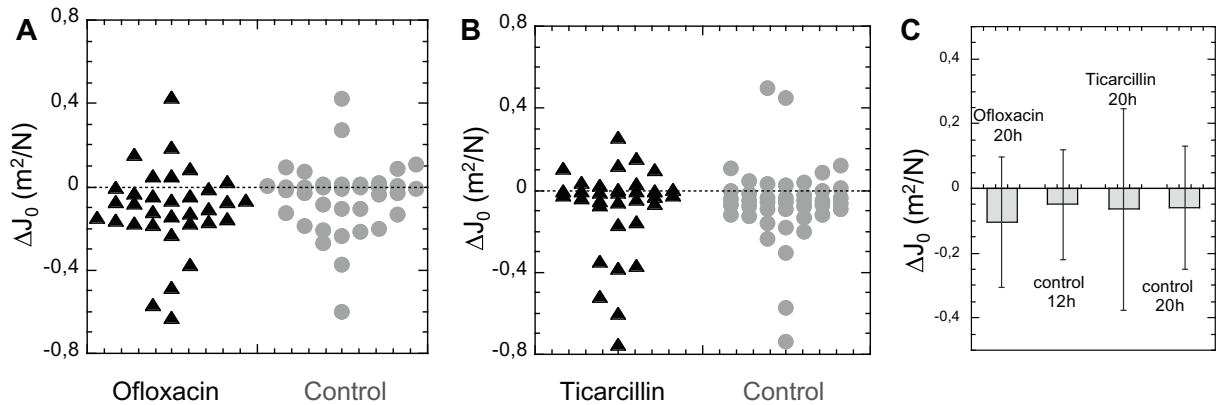


Figure 2. Elastic compliance changes caused by biofilm treatment with antibiotics. Elastic compliance differences $\Delta J_0 = (J_0(t_f) - J_0(t_i))$ recorded upon biofilm treatment with (A) ofloxacin $50 \mu\text{g ml}^{-1}$ for 12 h, (B) ticarcillin $800 \mu\text{g ml}^{-1}$ for 20 h (\blacktriangle) together with the corresponding controls treated the same way without antibiotics (\bullet). Each point is derived from one particle. The data shown are representative of three independent experiments. (C) The histogram gives the average of the differences measured in one biofilm. Error bars are standard deviations calculated over all the particles of the biofilm.

Table 2. Elastic compliance differences reported by the biofilm-embedded particles after antibiotic treatment.

| Elastic compliance differences | Mean | Standard deviation |
|--------------------------------|-------|--------------------|
| Ofloxacin | -0.1 | 0.2 |
| Control, 12 h | -0.05 | 0.18 |
| Ticarcillin | -0.07 | 0.31 |
| Control, 20 h | -0.06 | 0.19 |

20 h treatment of the biofilm with ofloxacin and ticarcillin, respectively. The corresponding controls run and measured in parallel in the absence of antibiotic are also shown in the same figure. Antibiotic-treated samples and control samples exhibited statistically identical distributions of the differences (figure 2 and table 2). The histogram in figure 2 summarizes the mean difference values all negative consistently with the tendency to stiffening that we have previously observed as biofilm ages (Galy *et al* 2012). We checked, looking at the relative difference of elastic compliance $\Delta J_0/J_0(t_i)$ that no effect possibly concentrated on the most rigid environments that would induce small absolute differences but large relative changes had been missed. Relative differences display larger spreading for low compliances—comprised between 1 and -1 for compliances below $0.3 \text{ m}^2 \text{ N}^{-1}$ and between -0.5 and 0.5 above—likely due to higher incertitude on the smallest values. However, the distribution of the values did not differ between treated samples and controls (plot shown in figure S2 (available from stacks.iop.org/NJP/15/125026/mmedia) for ofloxacin). As well, plotting the relative differences as a function of the biofilm depth showed no spatial dependence (data not shown). All the results stated that the changes measured on biofilms treated with antibiotics were similar to the ones

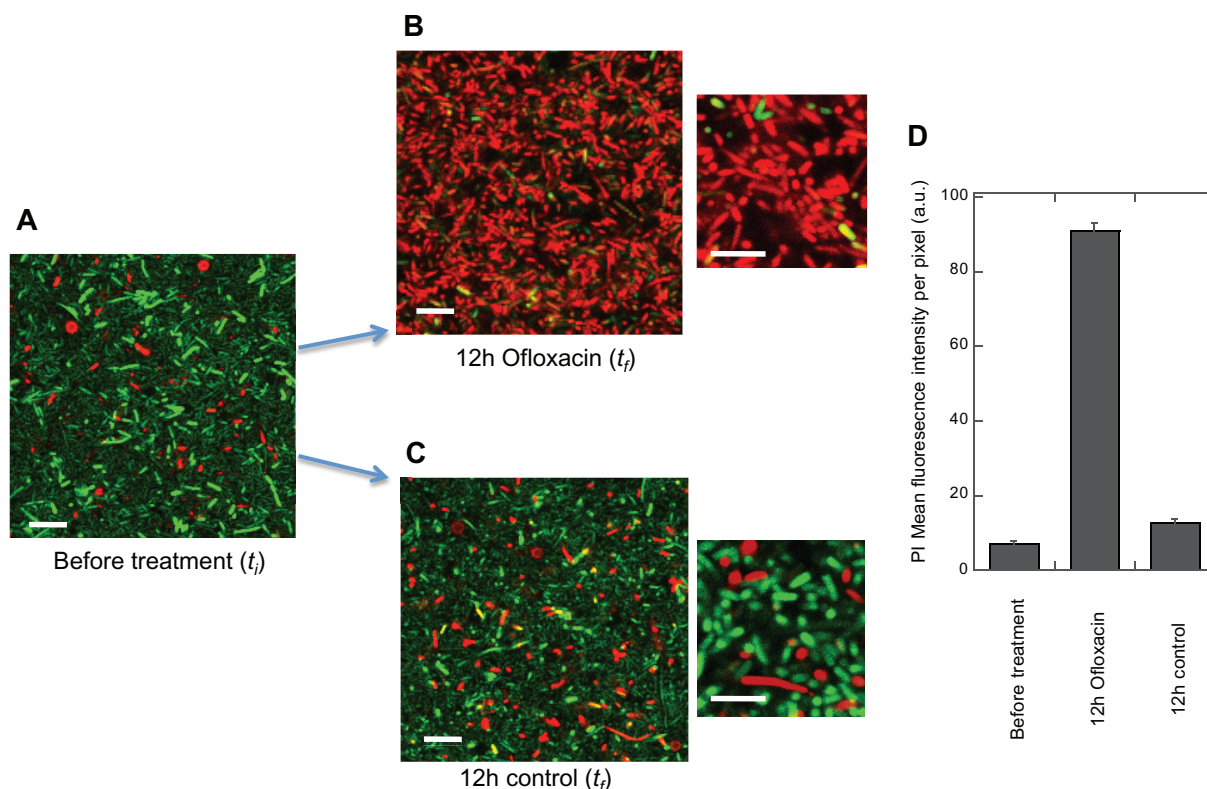


Figure 3. Confocal microscopy imaging of ofloxacin activity in biofilm. (A) Biofilm grown 24 h in standard conditions is labeled for 15 min with 20 μM PI before acquiring GFP (Exc 488; EM 520/20) and PI (Exc 561; EM 640/50) images (t_i). Same procedure is applied after (B) 12 h treatment of the biofilm with ofloxacin (t_f) and (C) 12 h nutrient flow without antibiotic as a control. HCX PL APo 63x/1.4-0.6 Oil immersion objective lens. The images shown here were collected at 8 μm from the flow cell bottom. Bars represent 10 μm ; small images correspond to a $\times 1.5$ zoom of the initial images. (D) Histogram of PI fluorescence intensities averaged on image series taken at 8 μm from the bottom of the flow cell before and after 12 h treatment with ofloxacin 50 $\mu\text{g ml}^{-1}$ or with medium without ofloxacin. Error bars are SDs from the image series.

measured on the control samples and fully explained by the material properties evolution as the biofilm ages. No significant alteration of the structure was induced by these high concentrations of antibiotics.

3.2.2. Antimicrobial activity. At that stage, we wished to verify the antibiotic biocidal activity in the biofilm conditions. To this purpose, we evaluated *in situ* the level of cell mortality using the dead cell marker, PI. This DNA-intercalating molecule does not penetrate living cells, labeling only bacteria with a compromised membrane, which reasonably correlates with cell death (Lehtinen *et al* 2004). Figure 3 shows confocal images recorded on biofilm with and without ofloxacin treatment and labeled with PI. The images show that biofilm grown for 20 h in standard conditions exhibited a residual level of cells permeable to PI characterized by a mean PI fluorescence intensity/pixel of 7 ± 0.9 au (images taken at biofilm height at 8 μm from the

bottom). This fluorescence significantly increased upon 12 h ofloxacin $50 \mu\text{g ml}^{-1}$ treatment, reaching 91 ± 2 au, which corresponded to almost all the cells exhibiting PI labeling. However, it should be mentioned that even in these conditions of high antibiotic concentration (800 MIC), a small amount of cells remained free of PI and still exhibiting GFP content. By counting locally on the PI and the GFP confocal images the number of GFP and PI labeled cells, we evaluated that $96 \pm 3\%$ of the cells were killed by ofloxacin treatment, showing that although the vast majority of the cells were killed, a small fraction of the cells remained alive. Similar results were obtained with ticarcillin (figure S3 (available from stacks.iop.org/NJP/15/125026/mmedia)) although PI fluorescence pattern exhibited an additional fuzzy fluorescent pattern suggesting that cells have released their internal content upon lysis. This is consistent with the ticarcillin mechanism of action targeting cell membrane. The percentage of dead cells was then more difficult to evaluate but very few cell still containing GFP were detected qualitatively indicating high cell mortality.

3.3. *Protease effect on biofilm mechanics*

To demonstrate the ability of our approach to evidence local mechanical changes induced by an external effector, we tested the effects of trypsin, an enzyme that cleaves proteins into pieces but does not enter into the cells preserving their viability over the time scale of a few hours. This experiment was inspired by our previous results indicating that extracellular polymer matrix cross-linking might essentially support biofilm mechanical properties (Galy *et al* 2012). The mechanical profile of the biofilm was determined before and after 1 h 30 min treatment with $500 \mu\text{g ml}^{-1}$ of trypsin. Figure 4 shows the variation of the elastic compliance induced by this treatment in a typical experiment. In contrast with what had been observed with antibiotics, trypsin-treatment-induced a significant increase of compliance in the biofilm. In addition, 20% of the particles initially recorded disappeared from the field of analysis which reported an environment of compliance greater than 0.1 Pa^{-1} , which had never been detected in untreated samples. These long-trajectory particles appeared to be randomly distributed in the biofilm and stemmed from initial environment with compliance values greater than 0.3 Pa^{-1} . Conversely, 25% of the particles reported small alterations remaining in the range of control's small changes. As for the particles removed from the field of observation, neither a defined location nor a given initial compliance value range were found for these environments protected from trypsin effects. The creep curve pairs recorded before and after trypsin treatment usually exhibited quasi-homothetic shapes (see examples in figure 4(C)) indicating that both elasticity and viscosity were jointly affected by trypsin treatment. Similarly, purely elastic signature was also conserved after trypsin treatment but with much higher elastic compliance values.

Bacterial viability was tested using PI labeling which remained at the level of the control—PI intensity found equal to 8 ± 1 au on the images taken at $8 \mu\text{m}$ from the biofilm bottom—confirming as expected that trypsin did not induce bacterial cell death at the concentration and at the time scale of our observations (figure S4 (available from stacks.iop.org/NJP/15/125026/mmedia)).

In a different set of experiments, we grew the biofilm in the presence of trypsin from the very beginning of the biofilm formation, just after initial surface colonization as we started nutrient flow. This treatment did not prevent biofilm formation but limited its height that was found equal to $20 \pm 2 \mu\text{m}$ in the presence of trypsin versus $38 \pm 4 \mu\text{m}$ in its absence. The biofilm formed in the presence of trypsin displayed much higher compliance arising from the increase

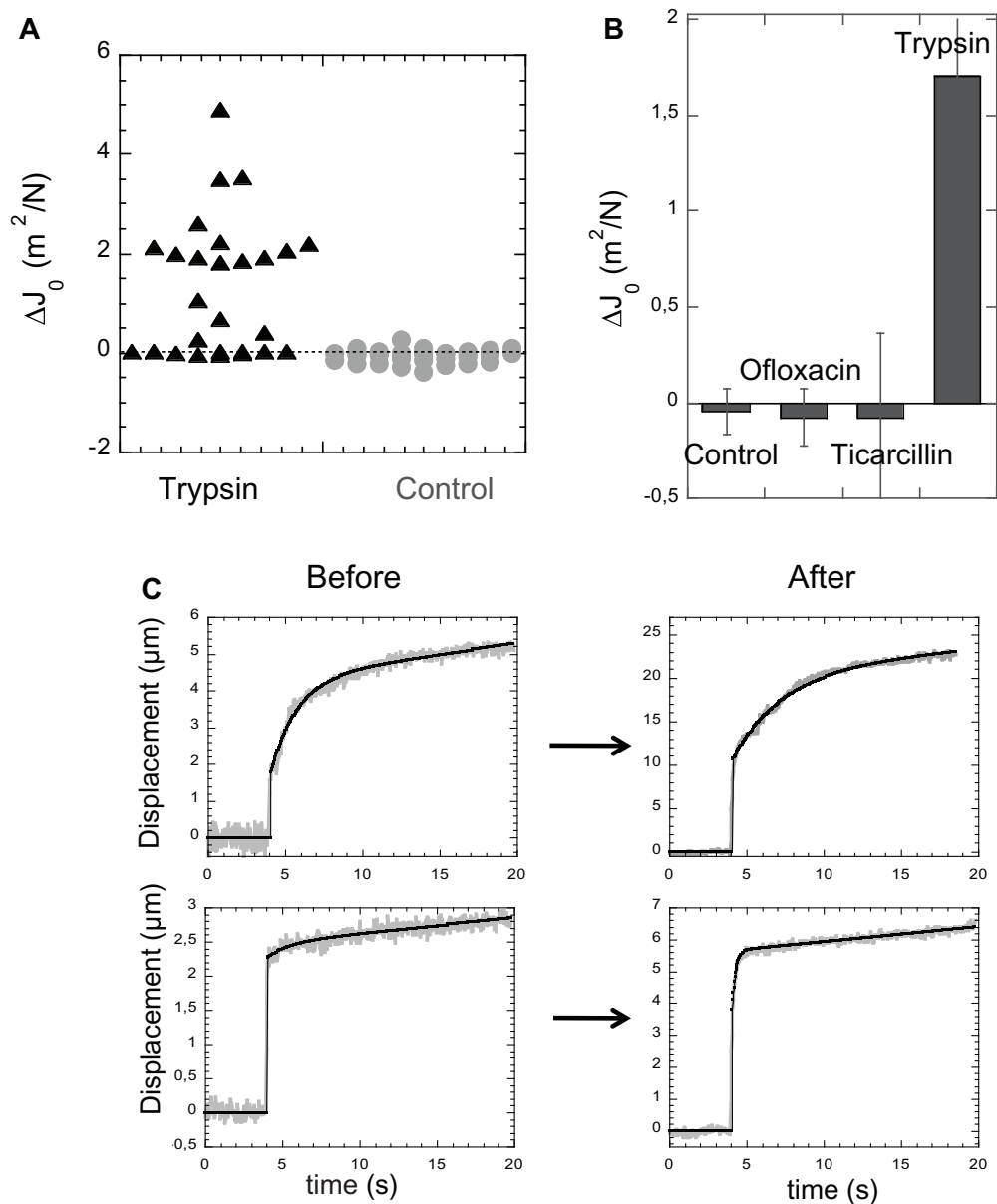


Figure 4. Trypsin-induced biofilm softening. (A) Elastic compliance differences recorded upon treatment with trypsin $500 \mu\text{g ml}^{-1}$ for 1 h 30 min of a 24 h biofilm grown at 0.3 ml h^{-1} nutrient flow rate (\blacktriangle) together with a control treated the same way in the absence of trypsin (\bullet). Each point is derived from one particle. (B) Histogram summarizing the effects induced by the three effectors used in this study; averaged values of elastic compliance difference are shown. (C) Typical pairs of creep curves obtained before and after trypsin treatment.

of both elastic contribution and viscous flow. Interestingly, this biofilm still exhibited a $10 \mu\text{m}$ bottom layer which averaged compliance— $J_0 = 0.3 \text{ m}^2 \text{ N}^{-1}$ —was significantly smaller than the one of the upper layer— $J_0 = 1.97 \text{ m}^2 \text{ N}^{-1}$. This bottom layer was nevertheless much softer than in the absence of trypsin.

These results showed that trypsin breaking or preventing protein links in the biofilm strongly affects its mechanical properties and that biofilm structural alterations were effectively detected by our approach.

4. Discussion and conclusions

The complex 3D biofilm organization creates a specific environment where biofilm bacteria exhibit properties absent in the planktonic mode of development. In the biofilm lifestyle, the role of the cell processes—triggered by bacterial immobilization and concentration on the surface, and the contribution of the specific physicochemical properties—generated by the 3D architecture and the confinement, are closely interwoven and are still far from being sorted out. The intrinsic spatial heterogeneity of bacterial biofilms, and the lack of microscale techniques giving access to local values in undisturbed biofilms still worsen the problem.

Recently, biofilm mechanical properties have been mainly described from a macroscopic material perspective, providing a large spectrum of values within apparently identical models and even within same sets of homogeneous experiments (Brindle *et al* 2011). This large scatter of the data does not help clarifying the causal relationships possibly linking the biofilm's physical and biological properties.

To gain insights into the understanding of the basic components supporting the biofilm's mechanical properties, investigating how they are impacted by various external stresses, including antibiotics, could be a particularly worthwhile strategy. A number of previous investigations have underlined the tolerance of bacterial biofilms to biocidal treatment and particularly to antibiotics. The involvement of different factors such as restricted penetration of antimicrobials, expression of specific resistance genes, mutations affecting antibiotic target, increased level of persisters, adaptation to stress, have been considered as possible factors of this resistance and widely reviewed (e.g. Stewart and Costerton 2001, Anderson and O'Toole 2008, Lewis 2008, Hoiby *et al* 2010). This question is still actively scrutinized all the more since the reduced susceptibility of biofilm bacteria to antimicrobial agents is a crucial problem in the treatment of chronic infections frequently involving biofilms (Costerton *et al* 1999, Potera 1999, Hoiby *et al* 2011).

The role of the extracellular polymeric substances (EPS) matrix itself in the biofilm tolerance to antibiotics is not clear. It might be very dependent on the organisms forming the structure. For instance, while a recent work has shown that *Bacillus subtilis* biofilms displayed non-wetting properties that should severely limit the penetration of antimicrobial liquids into the biofilm, other authors studying the vancomycin diffusion in *E. coli* biofilms have shown that the biofilm matrix was not an obstacle to the diffusion reaction of the antibiotic that can reach all cells through the biofilm (Daddi Oubekka *et al* 2012). The type of antimicrobial agents evaluated might also explain the significant differences observed (Stewart, 2003). Moreover, how antibiotics possibly affect the EPS matrix itself and what would be the impact of this on the biofilm resistance is not completely understood. To bring about clues to these questions we monitored the evolution of biofilm mechanical properties upon antibiotic treatment. Surprisingly, although antibiotics still remain the most common means of fighting infections, little work has been done to characterize the changes induced on biofilm architecture and mechanics upon antibiotics treatment. On the basis of macroscopic rheology measurements, Jones and co-workers (2011) reported weakening effects of ciprofloxacin in *P. aeruginosa* and of rifampicin in *S. epidermidis* biofilms while Lieleg and co-workers (2001) concluded

to the absence of effect of antibiotics including ofloxacin in several *Pseudomonas* species. Still, the biofilm architecture holds inherent heterogeneity and complexity which generates large variations in biofilm mechanical responses and important spreading of the data collected from material mean response (Brindle *et al* 2011). Therefore, the variations induced by specific effectors could easily be blurred in the scatter of data.

In the work described here, we took advantage of our recently developed technique enabling the *in situ* characterization of biofilm local mechanical properties, to clarify the effects of antibiotic treatment on biofilm structural organization. Our approach relies on the remote actuation of magnetic microparticles seeded in the three dimensions of the biofilm to report individually their local environment. Similarly, the different local mechanical microniches of a given biofilm can be evidenced and their spatial distribution precisely described. Moreover, we have shown in a previous paper that successive actuation runs could be performed without inducing mechanical response alteration. So here, we were able to investigate at the micron scale the potential effects of antibiotics on the biofilm micro-organization by recording the mechanical response of each particle located inside the biofilm before and after antibiotic treatment. We worked here with young biofilms grown in the presence of a low shear stress (approximately 10^{-3} Pa) displaying elastic modulus values comprised between 0.5 and 200 Pa. For the sake of comparison, *Streptococcus mutans* polysaccharides extracted from 5-day-old biofilm exhibit elastic moduli between 10^{-3} and 10^{-1} Pa depending on the stress frequency while the one found for bacterial cell wall has been found in the range of tens of kPa to MPa.

We did this for ticarcillin and ofloxacin, which were aimed at different cell targets, i.e. cell membrane through peptidoglycan polymerization inhibition and cell replication machinery through DNA-gyrase inhibition, respectively. The mechanical profile of the biofilm after 24 h growth, established before antibiotic treatment, displayed a heterogeneous distribution of visco-elastic parameter values differing by more than two orders of magnitude depending on spatial coordinates in the biofilm as previously shown (Galy *et al* 2012). None of the two antibiotics altered significantly this initial mechanical profile. Neither the nature of the material response to the mechanical stress—from purely elastic to visco-elastic with a relaxation time—nor the amplitude of the parameters were changed to a higher extent in the antibiotic-treated samples than in the controls. The elastic compliance differences only reported a slight stiffening of the material, which was characteristic of the biofilm ageing. In the mean time, antibiotic-treated biofilms stopped growing as shown by thickness increase arrest and PI-labeling results proved that most of the cells were killed after antibiotic treatment was applied.

Thereby, we demonstrate that mechanical properties revealed *in situ* at the micron scale are not affected by several hours of treatment at high antibiotic concentrations (800 MIC) which kill at least 95% of the cells. This is in good agreement with the observations of Lieleg and co-workers but tend to contradict other results that showed weakening effects of antibiotics (Jones *et al* 2011). This discrepancy might originate in the use of different bacterial species but might also be due to the difficulty in interpreting data from macroscopic rheology in a highly heterogeneous material. Nevertheless, the results of Jones and co-workers also stated the distinction between the killing power of an antimicrobial agent and its ability to alter biofilm mechanical properties which was also suggested in previous investigations dedicated to other biocides (Davison *et al* 2010, Brindle *et al* 2011, Lieleg *et al* 2011).

From our results, the mechanical properties appeared to remain unchanged upon cell death indicating that cell activity is not necessary for structure maintenance. To go further in the analysis of the biofilm mechanical property bases, it is worthwhile to consider the strong

analogy between biofilm mechanical properties and the ones of actin gels that have been extensively investigated. The large spreading of the values and the strong asymmetry of the distribution have been shown to originate in actin gels from high actin concentrations and a high degree of cross-linking of the gel by specific proteins such as fascin or scruin (Apgar *et al* 2000, Gardel *et al*, 2004). These observations prompted us to hypothesize that our *E. coli* biofilm structure similarly relies on a polymer network cross-linking in which proteins play a crucial roles.

To test this hypothesis and validate our approach using a biofilm effector that actually affected its physical properties, we have tested here the effect of trypsin, a protein-hydrolyzing enzyme that preserves cell viability. By contrast with antibiotic treatment, infusing a biofilm with this proteolytic enzyme had a large effect on biofilm mechanics significantly increasing the local compliance throughout the three dimensions of the biofilm. These results evidence a rise of the elastic compliance, reflecting—as described by semi-flexible polymer scaling relations (MacKintosh *et al* 1995)—an increase of polymer mesh size and of the averaged distance between the cross-links due to the decrease of the number of cross-links of network. We also observed an increase in the viscous flow upon trypsin treatment suggesting that the removal of the tightest links expose softer cross-linking such as polymer entanglement. However, randomly distributed islets in the biofilm remained mechanically unchanged by trypsin treatment; they displayed no particular initial compliance range of values. This might correspond to biofilm niches structured by different factors such as multivalent ions or tighter polymer entanglement. Our results show that cleavage of extracellular proteins lead to a profound remodeling of the biofilm. Consistently, multivalent ions or cross-linking agents such as glutaraldehyde have been shown to stiffen biofilms of several micro-organisms (Stoodley 2001; Wloka 2004; Ahimoe 2007; Mohle 2007, Lieleg 2011) while divalent cations chelating agents promote the eradication of mature biofilms *in vivo* (Chauhan *et al* 2012).

Interestingly, introducing trypsin at the beginning of the biofilm growth just after the initial adhesion step on the flow cell bottom did not prevent biofilm growth although the thickness of the attached layer was lower. The material exhibited significantly higher compliance values in all the dimensions of the biofilm confirming that extracellular proteins acting as polymer cross-linkers represent a key factor of this *E. coli* biofilm structuration and stabilization. This corroborates the findings of other authors having previously recognized the effects of proteases on biofilm formation (Chaignon *et al* 2007, Gilan and Sivan 2013). Boles and Horswill even proposed that protease secretion by the constituting cells might be involved in the community self-controlled dispersion (Boles *et al* 2010). Our results suggest that the dispersion is induced by the enzymatic breaking of the extracellular polymer network cross-linkers.

In summary, we have used our recently developed magnetic particle remote actuation approach to investigate *in situ* the effects of antibiotic treatment on the mechanical properties of an established *E. coli* biofilm. We have demonstrated that antibiotics, although killing the majority of the cells, did not alter the biofilm's physical properties, preserving its integral spatial organization and solidity. This should provide a remarkable advantage for the persister cells present in all bacterial populations (Lewis 2010, Balaban 2011) and especially in biofilm (Lewis 2008)—the shelter built by the ancestor cells remaining safe and sound, ready to promote persister cells resilience at any favorable condition change. This underlines that conventional bacteria control relying on the use of biocides targeting cells is missing a key target in the fight against biofilm. We have also shown here that a non-toxic effector, enabling to break biofilm cross-linkers on which biofilm architecture seems to rely can be much more efficient in

destabilizing the edifice. We believe that further insights in the unveiling of the origin of biofilm mechanical properties are needed to make significant progress in biofilm control strategies. Our results promote an approach consisting the combining of local mechanics analysis and the use of biofilm effectors targeting the polymer network to eventually reveal the biofilm microstructure locks and find new strategies to specifically release them.

References

- Aggarwal S, Poppele E H and Hozalski R M 2010 Development and testing of a novel microcantilever technique for measuring the cohesive strength of intact biofilms *Biotechnol. Bioeng.* **105** 924–34
- Anderson G G and O'Toole G A 2008 Innate and induced resistance mechanisms of bacterial biofilms *Curr. Top. Microbiol. Immunol.* **322** 85–105
- Apgar J, Tseng Y, Fedorov E, Herwig M B, Almo S C and Wirtz D 2000 Multiple-particle tracking measurements of heterogeneities in solutions of actin filaments and actin bundles *Biophys. J.* **79** 1095–106
- Aravas N and Laspidou C S 2008 On the calculation of the elastic modulus of a biofilm streamer *Biotechnol. Bioeng.* **101** 196–200
- Balaban N Q 2011 Persistence: mechanisms for triggering and enhancing phenotypic variability *Curr. Opin. Genet. Dev.* **21** 768–75
- Bausch A R, Ziemann F, Boulbitch A A, Jacobson K and Sackmann E 1998 Local measurements of viscoelastic parameters of adherent cell surfaces by magnetic bead microrheometry *Biophys. J.* **75** 2038–49
- Bernier S P, Lebeaux D, Defrancesco A S, Valomon A, Soubigou G, Coppee J Y, Ghigo J M and Beloin C 2013 Starvation, together with the SOS response, mediates high biofilm-specific tolerance to the fluoroquinolone ofloxacin *PLoS Genet.* **9** e1003144
- Boles B R, Thoendel M, Roth A J and Horswill A R 2010 Identification of genes involved in polysaccharide-independent *Staphylococcus aureus* biofilm formation *PLoS ONE* **5** e10146
- Brindle E R, Miller D A and Stewart P S 2011 Hydrodynamic deformation and removal of *Staphylococcus epidermidis* biofilms treated with urea, chlorhexidine, iron chloride, or dispersinB *Biotechnol. Bioeng.* **108** 2968–77
- Cense A W, Peeters E A, Gottenbos B, Baaijens F P, Nuijs A M and Van Dongen M E 2006 Mechanical properties and failure of *Streptococcus mutans* biofilms, studied using a microindentation device *J. Microbiol. Methods* **67** 463–72
- Chaignon P, Sadovskaya I, Ragunah C, Ramasubbu N, Kaplan J B and Jabbouri S 2007 Susceptibility of staphylococcal biofilms to enzymatic treatments depends on their chemical composition *Appl. Microbiol. Biotechnol.* **75** 125–32
- Chauhan A, Lebeaux D, Ghigo J M and Beloin C 2012 Full and broad-spectrum in vivo eradication of catheter-associated biofilms using gentamicin-EDTA antibiotic lock therapy *Antimicrob. Agents Chemother.* **56** 6310–8
- Costerton J W, Stewart P S and Greenberg E P 1999 Bacterial biofilms: a common cause of persistent infections *Science* **284** 1318–22
- Daddi Oubekka S, Briandet R, Fontaine-Aupart M P and Steenkeste K 2012 Correlative time-resolved fluorescence microscopy to assess antibiotic diffusion-reaction in biofilms *Antimicrob. Agents Chemother.* **56** 3349–58
- Davison W M, Pitts B and Stewart P S 2010 Spatial and temporal patterns of biocide action against *Staphylococcus epidermidis* biofilms *Antimicrob. Agents Chemother.* **54** 2920–7
- Galy O, Latour-Lambert P, Zrelli K, Beloin C, Ghigo J M and Henry N 2012 Mapping of bacterial biofilm local mechanics by magnetic microparticle actuation *Biophys. J.* **5** 1400–8
- Gardel M L, Shin J H, Mackintosh F C, Mahadevan L, Matsudaira P and Weitz D A 2004 Elastic behavior of cross-linked and bundled actin networks *Science* **304** 1301–5
- Ghigo J M 2001 Natural conjugative plasmids induce bacterial biofilm development *Nature* **412** 442–5
- Gilan I and Sivan A 2013 Effect of proteases on biofilm formation of the plastic degrading actinomycete *Rhodococcus ruber* C208 *FEMS Microbiol. Lett.* **342** 18–23

- Hoiby N, Bjarnsholt T, Givskov M, Molin S and Ciofu O 2010 Antibiotic resistance of bacterial biofilms. *Int. J. Antimicrob. Agents* **35** 322–32
- Hoiby N, Ciofu O, Johansen H K, Song Z J, Moser C, Jensen P O, Molin S, Givskov M, Tolker-Nielsen T and Bjarnsholt T 2011 The clinical impact of bacterial biofilms *Int. J. Oral Sci.* **3** 55–65
- Jones W L, Sutton M P, Mckittrick L and Stewart P S 2011 Chemical and antimicrobial treatments change the viscoelastic properties of bacterial biofilms *Biofouling* **27** 207–15
- Klapper I, Rupp C J, Cargo R, Purvedorj B and Stoodley P 2002 Viscoelastic fluid description of bacterial biofilm material properties. *Biotechnol. Bioeng.* **80** 289–96
- Korstgens V, Flemming H C, Wingender J and Borchard W 2001 Uniaxial compression measurement device for investigation of the mechanical stability of biofilms *J. Microbiol. Methods* **46** 9–17
- Lau P C, Dutcher J R, Beveridge T J and Lam J S 2009 Absolute quantitation of bacterial biofilm adhesion and viscoelasticity by microbead force spectroscopy *Biophys. J.* **96** 2935–48
- Lehtinen J, Nuutila J and Lilius E M 2004 Green fluorescent protein-propidium iodide (GFP-PI) based assay for flow cytometric measurement of bacterial viability *Cytometry A* **60** 165–72
- Lewis K 2008 Multidrug tolerance of biofilms and persister cells *Curr. Top. Microbiol. Immunol.* **322** 107–31
- Lewis K 2010 Persister cells *Annu. Rev. Microbiol.* **64** 357–72
- Lieleg O, Caldara M, Baumgartel R and Ribbeck K 2011 Mechanical robustness of *Pseudomonas aeruginosa* biofilms *Soft Matter* **7** 3307–14
- Mackintosh F C, Kas J and Janmey P A 1995 Elasticity of semiflexible biopolymer networks *Phys. Rev. Lett.* **75** 4425–8
- Perkins G S and Jones R B 1991 Hydrodynamic interaction of a spherical particle with a planar boundary: I. Free surface *Physica A* **171** 575–604
- Perkins G S and Jones R B 1992 Hydrodynamic interaction of a spherical-particle with a planar boundary: 2. Hard-wall *Physica A* **189** 447–77
- Poppele E H and Hozalski R M 2003 Micro-cantilever method for measuring the tensile strength of biofilms and microbial flocs *J. Microbiol. Methods* **55** 607–15
- Potera C 1999 Forging a link between biofilms and disease *Science* **283** 1837–9
- Sbalzarini I F and Koumoutsakos P 2005 Feature point tracking and trajectory analysis for video imaging in cell biology *J. Struct. Biol.* **151** 182–95
- Schnurr B, Gittes F, Mackintosh F C and Schmidt C F 1997 Determining microscopic viscoelasticity in flexible and semiflexible polymer networks from thermal fluctuations *Macromolecules* **30** 7781–92
- Shaw T, Winston M, Rupp C J, Klapper I and Stoodley P 2004 Commonality of elastic relaxation times in biofilms *Phys. Rev. Lett.* **93** 0988102
- Stewart P S 2003 Diffusion in biofilms *J. Bacteriol.* **185** 1485–91
- Stewart P S and Costerton J W 2001 Antibiotic resistance of bacteria in biofilms *Lancet* **358** 135–8
- Stewart P S and Franklin M J 2008 Physiological heterogeneity in biofilms *Nature Rev. Microbiol.* **6** 199–210
- Stoodley P, Lewandowski Z, Boyle J D and Lappin-Scott H M 1999 Structural deformation of bacterial biofilms caused by short-term fluctuations in fluid shear: an in situ investigation of biofilm rheology *Biotechnol. Bioeng.* **65** 83–92
- Towler B W, Rupp C J, Cunningham A B and Stoodley P 2003 Viscoelastic properties of a mixed culture biofilm from rheometer creep analysis *Biofouling* **19** 279–85